

Electronic Supplementary Information

Broad spectrum photoluminescence quaternary quantum dots for cell and animal imaging

Dawei Deng,^{*a,b} Lingzhi Qu,^a Samuel Achilefu^c and Yueqing Gu^{*a}

^a School of Life Science and Technology, China Pharmaceutical University, Nanjing 210009, China. Fax: (+86)-25-83271046; Tel: (+86)-25-83271080; E-mail: dengdawei@cpu.edu.cn or dengd@umich.edu, guyueqingsubmission@hotmail.com

^b Chemical Engineering Department, University of Michigan, Ann Arbor, Michigan 48109, United States

^c Department of Radiology, School of Medicine, Washington University, St. Louis, Missouri 63110, United States

EXPERIMENTAL SECTION

Materials. Zinc acetate ($\text{Zn}(\text{Ac})_2$, 99.99%), silver nitrate (AgNO_3 , 98+%), indium acetate ($\text{In}(\text{Ac})_3$, 99.99%), Se powder (100 mesh, 99.5%), 1-octadecene (ODE, 90%), oleic acid (OA, 90%), 1-dodecanethiol (DDT, 98%), oleylamine (OLA, 97%), n-decane (98%), rhodamine B (RhB). The NIR dye-cypate was provided by prof. Samuel Achilefu.^{1,2} In addition, folate-modified N-succinyl-N'-octyl-chitosan (FA-SOC) micelles used for the water transfer of oil-soluble QDs were synthesized according to our previous reports.^{3,4} All chemicals were used without further purification. The water used in all experiments had a resistivity higher than $18.2 \text{ M}\Omega\cdot\text{cm}$.

Human hepatoma cell line (Bel-7402) and human lung carcinoma cell line (A549) were purchased from American Type Culture Collection (ATCC, Manassas, VA, USA). Athymic nude mice (nu/nu, half male and half female; aged 4–6 weeks and weighed at 18–20 g) were purchased from Charles River Laboratories (Shanghai, China). (Folate-free) RPMI 1640 medium, calf serum, penicillin, streptomycin, trypsin, and EDTA were purchased from commercial sources.

Synthesis of Quaternary ZnAgInSe_3 QDs. For a typical synthetic reaction, $\text{Zn}(\text{Ac})_2$ (0.1 mmol), AgNO_3 (0.1 mmol), and $\text{In}(\text{Ac})_3$ (0.1 mmol) were mixed with 4 mL of ODE, 0.5 mL of DDT and 50 μL of OA in a 50 mL three-neck flask. The reaction mixture was heated to 175°C for 10 min under N_2 flow with mild stirring until a clear solution was formed. At this

time, the Se precursor solution prepared by dissolving 0.3 mmol of Se powder in the mixture of oleylamine (0.5 mL) and dodecanethiol (0.2 mL)⁵ was injected with a syringe. The solution turned immediately to dark. The reaction temperature was retained at this temperature for 30 min to allow the growth of ZnAgInSe₃ QDs. After that, the flask was rapidly cooled to room temperature to harvest QDs products. The resulting QDs could be isolated by precipitating with ethanol, centrifuging and decanting the supernatant. The residue could be re-dispersed in n-decane, toluene, hexane, chloroform, ether, etc. In this study, we explored the effect of the reaction temperature, the growth time, the amount of DDT and the Zn/Ag feed ratio on the synthesis of the quaternary QDs. XRD, TEM, EDAX and XPS measurements were performed to characterize the crystallinity, size and elemental composition of the QDs.

Synthesis of Folate-modified N-succinyl-N'-octyl-chitosan (FA-SOC) Micelles. FA-SOC micelles were synthesized using a two-step method reported previously.^{3,4}

Preparation of SOC Micelles. Briefly, chitosan (1 g) was reacted with succinic anhydride (3 g) in acetone (17 mL) for 48 h with constant stirring at room temperature to produce N-succinyl-chitosan, followed by precipitation with 1 M NaOH solution, centrifugation, and washing procedures using alcohol. After decantation, the precipitate of N-succinyl-chitosan was dried under vacuum at 60 °C overnight. Next, N-succinyl-chitosan (1 g) was further reacted with octaldehyde (1.02 g) in acetic acid solution. After constant stirring for 4 h, NaBH₄ (0.16 g) solution was added dropwise to the mixture and reacted for another 12 h, followed by neutralization with 1 M NaOH and purification by dialysis (molecular weight cut off (MWCO) 10000). After lyophilization, the SOC powder was obtained.

Folate Modification of SOC Micelles. The γ -COOH group of folic acid (22 mg) was activated by DCC/NHS catalyst systems (molar ratio of folate:DCC:NHS = 1:1.2:2) in anhydrous dimethyl sulfoxide (DMSO, 2.5 mL) under mild stirring in the dark for 12 h at room temperature. Then, the activated folic acid was added dropwise into the SOC solution, and reacted with the free amino group on the surface of micelles to form folate-modified SOC micelles. The product was purified by dialysis (MWCO 10000) against distilled water for subsequent study. The degree of modification of the amino groups in the chitosan molecule by octaldehyde, folate and succinic anhydride has been provided in our recent report.³

QD Solubilization in Water with FA-SOC Micelles. The quaternary ZAISe QDs was transferred into water by micelle encapsulation, as described in Ref. 3: Typically, 50 μ L of the quaternary QDs (~0.6 mg) was precipitated with ethanol to remove excess unreacted precursors and re-dispersed in 50 μ L of chloroform. The QDs were then mixed with 1 mL of FA-SOC micelles (5 mg) water solution by sonication in cold-water bath. At room temperature, the chloroform was gradually evaporated, yielding a slightly turbid solution. After centrifugation, the lipid QDs-loaded FA-SOC micelles in water solution was obtained and kept at room temperature for further use.

Characterization of QDs and QDs-loaded Micelles. An S2000 eight-channel optical fiber spectrophotometer (Ocean Optics corporation, America), a broadband light source (X-Cite Series 120Q, Lumen Dynamics Group Inc., Canada) and two Fiber Coupled Laser Systems (λ =660 and 766 nm, Enlight, China) were utilized for the detection of fluorescence spectrum.

A PerkinElmer UV/Vis spectrometer was employed for the measurement of UV–Vis spectrum. All above optical measurements were performed at room temperature. The fluorescence lifetime study was carried out at room temperature using an Edinburgh FLS 920 single-photon counting system (Edinburgh instruments, Britain) with excitation at 405 nm (EPL-405 picosecond pulsed Laser). PL QY of QDs in n-decane was calculated by comparing their integrated emission to that of rhodamine B (QY=90%, absolute ethanol, λ_{ex} =515 nm, 10 °C) or cypate (QY, 12%).^{1–3,6} Optical densities of all solutions at the excitation wavelength were less than 0.1 in order to measure truly the PL spectra of QDs.

TEM images were taken on a JEOL JEM-2100 transmission electron microscope with an acceleration voltage of 200 kV. Carbon-coated copper grids were dipped in the decane solution to deposit QDs onto the film. Elemental compositions of QDs were determined by energy-dispersive spectroscopy (EDS) and X-ray photoelectron spectroscopy (XPS, PHI5000 VersaProbe, ULVAC-PHI Inc., Japan). Powder XRD measurement was carried out using a Philips X'Pert PRO X-ray diffractometer. XRD samples were prepared by evaporating the concentrated QD ethanol suspension on a small glass plate. The size and morphology of micelles and QDs-loaded micelles were characterized by Mastersizer 2000 Laser Particle Size Analyzer (LPSA, Malvern, British), combined with TEM.

***In vitro* Cell Microscopy Imaging.** Bel-7402 cells were cultured in folate-free RPMI 1640 medium with 10% (v/v) calf serum at 37 °C (5% CO₂) and grown in a 24-well plate. After seeding for 24 h, the medium was aspirated, and then 0.5 mL of fresh folate-free RPMI 1640 medium containing QDs-loaded FA-SOC micelles ([QDs]≈10 µg/mL) was added to the wells. After incubation for 12 h, the medium was aspirated and the cells were washed with PBS three times for 5 min each. The fluorescence images of the cells were obtained with an Olympus Fluoview 300 confocal laser scanning system with 488 nm argon laser excitation.

***In vivo* NIR Fluorescence Imaging.** *In vivo* NIR Fluorescence imaging of the QDs-loaded FA-SOC micelles in tumor-bearing nude mice was performed with an in-house-built small animal NIR imaging system (laser source, Fiber Coupled Laser Systems (λ =660 and 766 nm, Enlight, China); detector, high sensitive NIR CCD camera (PIXIS 512B, Princeton Instrument, America)), which has been described in detail in our previous reports.^{3,4,7} All animal studies conform to the policies in the Animal Management Rules of the Ministry of Health of the People's Republic of China (document no. 55, 2001) and the guidelines for the Care and Use of Laboratory Animals of China Pharmaceutical University. Briefly, the Bel-7402 cells were injected subcutaneously in the right armpit of each nude mouse. After the tumors reached about 0.5 cm in diameter, the mice were used for *in vivo* imaging studies. In a typical imaging experiment, mice (n=3 for each group) were injected intravenously with QDs-loaded FA-SOC micelles (the dose of QDs, ~10 µg/g body weight), and imaged at various time points (0–12 h) post-injection. All fluorescence images were acquired with 300 ms exposure.

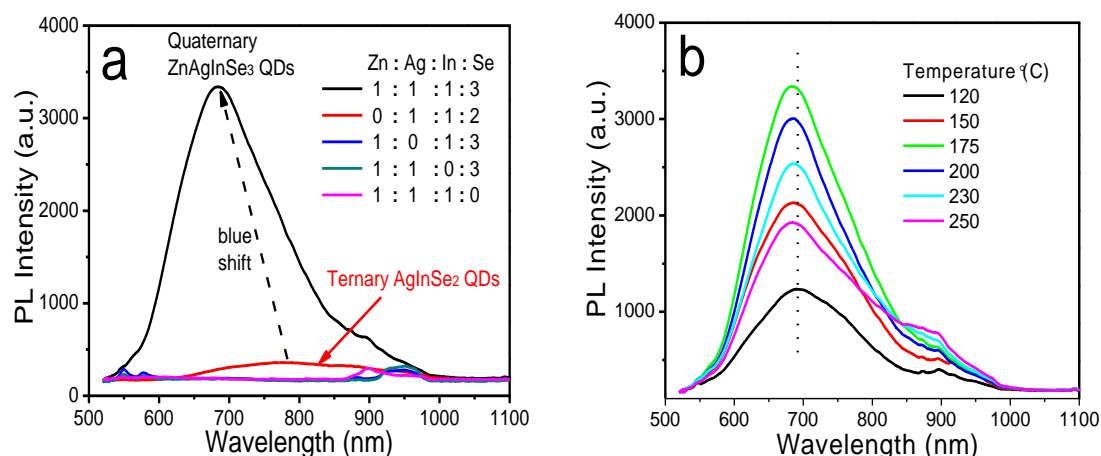


Fig. S1 (a) Photoluminescence (PL) spectra of the dispersions prepared with different Zn/Ag/In/Se feed ratios, in which Se powder dissolved in the mixture of oleylamine (OLA) and 1-dodecanethiol (DDT) was used as Se source (selenium can be reduced by DDT, and further associates with OLA to form the OLA–Se complexes⁵). In this quaternary system, the absence of Zn from the reaction mixture results in a significant decrease in PL intensity of QDs, whereas in the absence of any one of In, Ag and Se, no PL emission is observed. This indicates that the host QDs should be composed of an alloy of Zn, Ag, In and Se, namely, the formation of quaternary ZnAgInSe₃ QDs. And as compared with ternary AgInSe₂ QDs ($\lambda_{em} \sim 800$ nm), the PL peak ($\lambda_{em} = 685$ nm) of the QDs formed in the quaternary system blue-shift greatly, which further confirms the formation of quaternary ZAISe QDs (the band gaps of bulk AgInSe₂ and ZnSe are 1.24 and 2.7 eV, respectively).^{8,9}

(b) Temporal evolution of PL spectra of quaternary ZAISe QDs synthesized during a programmed heating process (rate: ~ 3 °C/min), in which the Zn/Ag/In/Se feed ratio was fixed at 1:1:1:3. As reported in previous literatures,^{8,10} an obvious challenge for the fabrication of ternary I–III–VI or quaternary Zn–I–III–VI semiconductors nanocrystals is their ternary or quaternary compositions, compared with the common binary II–VI and III–V nanocrystals. As such, balancing the reactivity of several cationic precursors is critical for the control of the stoichiometric ratio of the compositions in a given sample. In this study, we use the reactivity-controlling ligand–dodecanethiol reported by Peng et al.¹⁰ for cationic precursors (Ag and In), since the silver and indium had higher reactivity than zinc in the reaction with selenium in our synthesis system.¹¹ The data in panel b indicate that (i) the OLA–Se complexes formed by dissolving Se powder in the mixture of OLA and DDT are highly reactive. It is found that even at 90 °C, the OLA–Se complexes can react with Zn²⁺, Ag⁺ and In³⁺ to form quaternary ZAISe QDs. (ii) And with the increase of reaction temperature from 120 to 250 °C, no obvious blue-shift in the PL peak of QDs is observed, which suggests that homogeneous quaternary ZAISe nuclei with certain compositions are formed directly by the reaction between cations and selenium.¹² That is to say, the growth process that AgInSe₂ nucleates first, subsequently zinc gradually diffuses into QDs in the crystal growth stage should not be the principal formation mechanism of quaternary ZAISe QDs in our synthesis system (the band gaps of bulk AgInSe₂ and ZnSe are 1.24 and 2.7 eV, respectively^{8,9}).^{8,13,14}

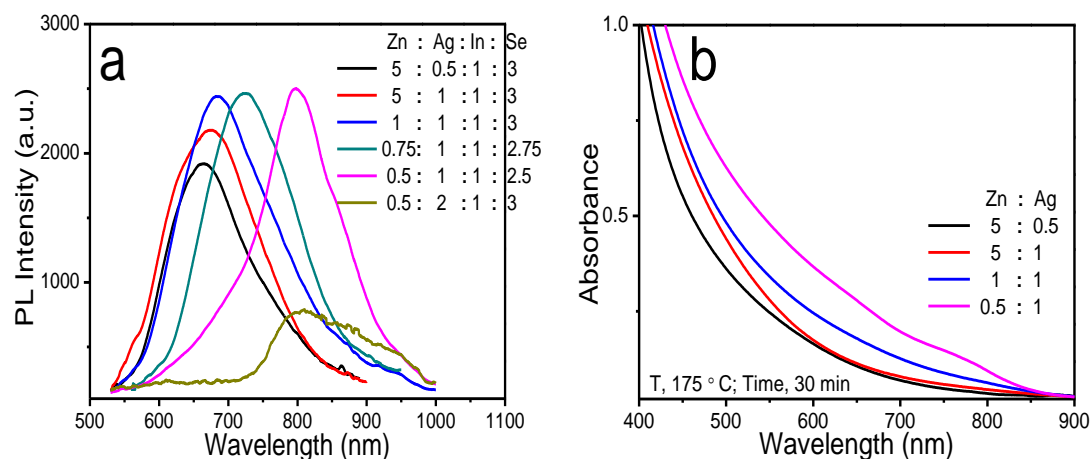


Fig. S2 (a) PL and (b) absorption spectra of the dispersions of the quaternary ZAlSe QDs with different Zn/Ag feed ratios prepared under 175 °C for 30 min. As shown, by changing the Zn/Ag feed ratio from 5:0.5 to 0.5:2, the PL peak of the resulting quaternary ZAlSe QDs can be conveniently tuned from 660 nm to 800 nm (the maximal PL QY is close to ~50% (PL peak, 675 nm)), and the corresponding absorption spectra also red-shift gradually. TEM observation indicated that all of the samples had a similar particle size (~5 nm in diameter), which could exclude the size effect on the shift of the band edges. Thus, the spectral shifts induced by the change of the Zn/Ag feed ratio should be attributed to the resultant variation in the composition of the QDs, which has been proven by the elemental analyses from EDX and XPS. This result further proves that different with the binary II–VI and III–V QDs, for quaternary Zn–I–III–VI semiconductors QDs, their compositions might play a more important role in determining the PL peak position, as observed recently by us and other groups.^{8,12,15} In addition, the PL and absorption spectra of the quaternary ZAlSe QDs are found to be broad and structureless (i.e., no well-defined exciton absorption peak), respectively, although the as-produced QDs have a narrow size distribution as shown in Fig. S3a. These also are the typical indicative features of quaternary compounds, which should be attributed to the unique electronic properties and the inhomogeneity of elemental distribution among different quaternary QDs in an ensemble.^{3,8,12–15}

In the present study, other crucial experimental variables, such as the reaction temperature (Fig. S1b), the reaction time and the amount of DDT used were also orderly varied to systematically investigate their influence on the PL properties of the resulting quaternary ZAlSe QDs. Our results show that the reaction temperature of 175 °C, the reaction time of 30 min and the DDT amount of 0.7 mL (namely, 0.5+0.2) are optimal for achieving the highly luminescent quaternary ZAlSe QDs.

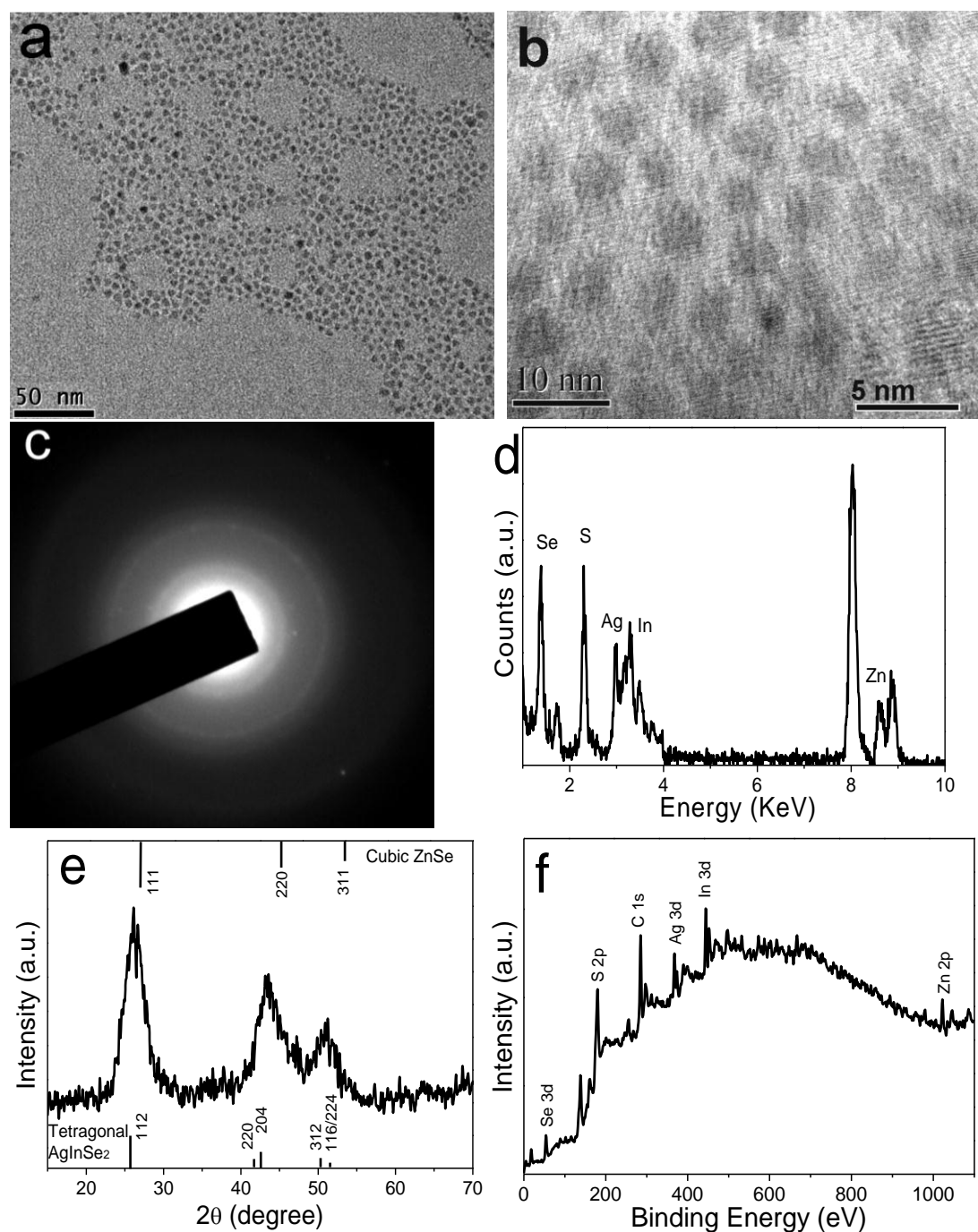


Fig. S3 (a) TEM image, (b) High-resolution TEM image, (c) selected area electron diffraction (SAED) pattern, and (d) the corresponding EDX spectrum of quaternary ZnAgInSe_3 QDs (the Zn/Ag/In/Se feed ratio was 1:1:1:3). (e) Typical XRD pattern and (f) XPS spectrum of oil-soluble quaternary ZnAgInSe_3 QDs. TEM image in part a shows that the as-produced QDs have a narrow size distribution (the diameter, 5 nm). The data in parts b, c and e indicate that the obtained quaternary QDs had a cubic crystal structure (zinc blende). The three major diffraction peaks were generally in between the main XRD peaks of chalcopyrite AgInSe_2 and cubic ZnSe . Quantitative elemental analyses of the QDs by EDX and XPS in parts d and f confirm that in this case, the compositions of the QDs were well consistent with the molar

ratios of the precursors used, indicating the formation of Zn-Ag-In-Se QDs.

In summary, based on the experimental results in Figures S1–S3, high-quality quaternary ZAlSe QDs have been prepared in the present study. And several significant conclusions could be drawn: (i) homogeneous quaternary ZAlSe QDs are formed directly by the reaction between cations and selenium dissolved in the mixture of OLA and DDT with the assistance of the cation reactivity-controlling ligand–dodecanethiol; (ii) the compositions of the QDs could be tuned by controlling the molar ratio of the Zn/Ag feed ratio used, which determine the PL peak position of these quaternary QDs. That is, by introducing Zn ions, quaternary ZAlSe alloy QDs would be formed *via* alloying the wider band gap ZnSe (2.7 eV) with a narrower band gap AgInSe₂ (1.24 eV). And the bandgap of ZAlSe QDs will be larger with more Zn ions introduced (i.e., the increase of Zn content in the QDs); (iii) finally, the as-produced quaternary QDs have a narrow size distribution and a high PL QY.

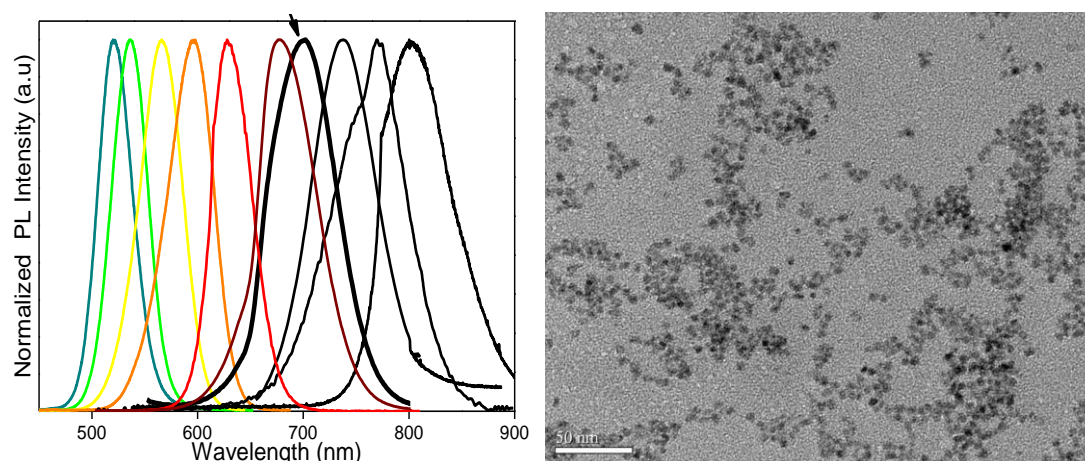


Fig. S4 Left: PL spectra of the as-prepared aqueous *N*-acetyl-L-cysteine(NAC)-capped binary CdTe QDs.¹⁶ As shown, by controlling the reaction time and the reaction temperature, the PL peak of the resulting binary CdTe QDs could be tuned from 520 nm to 800 nm (Full width at half-maximum (FWHM): 35–80 nm). The CdTe QDs with the PL spectrum labeled by arrow was used as the control (the binary QDs) in this study. Right: The typical TEM image of the as-prepared aqueous CdTe QDs. These aqueous binary QDs have a good monodispersity.

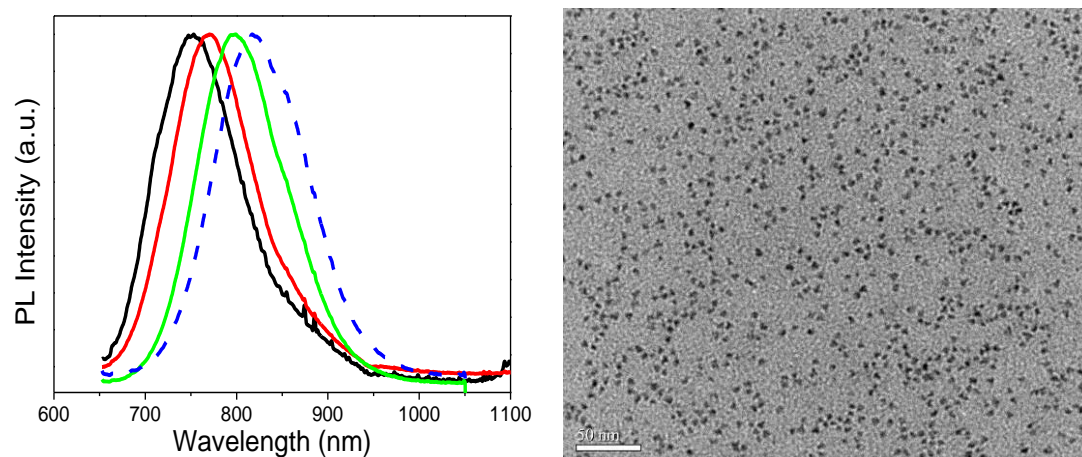


Fig. S5 Left: PL spectra of the as-prepared oil-soluble oleic acid (OA)-capped binary PbS QDs.¹⁷ As shown, by controlling the reaction time, the PL peak of the resulting binary PbS QDs could be tuned from 750 nm to 820 nm (FWHM: 110–120 nm). In this study, the PbS QDs was not used as the control (the binary QDs) since up to now, 700 nm-emitting PbS QDs have not been prepared. Right: The typical TEM image of the as-prepared oil-soluble PbS QDs. These oil-soluble binary QDs have a good monodispersity.

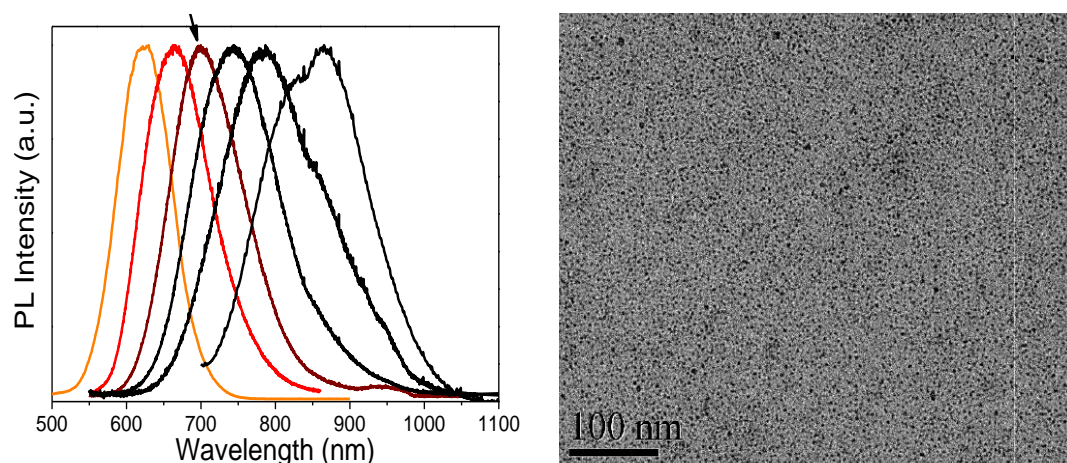


Fig. S6 Left: PL spectra of the as-prepared oil-soluble DDT-capped ternary Cu-In-S (CIS) QDs.³ As shown, the PL peak of the resulting ternary CIS QDs could be tuned from 620 nm to 870 nm (FWHM: 85–165 nm). In the present study, the CIS (and CIS/ZnS) QDs with the PL emission at ~700 nm (as labeled by arrow) were used as the control (the ternary QDs). Right: The typical TEM image of the as-prepared oil-soluble CIS QDs. These oil-soluble ternary QDs have a narrow size distribution.

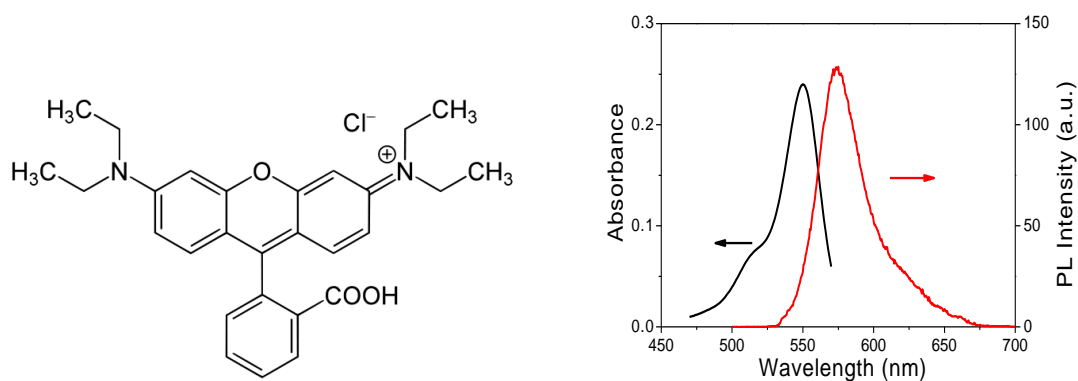


Fig. S7 Left: The molecular structure of rhodamine B. Right: Absorption and PL spectra of rhodamine B.

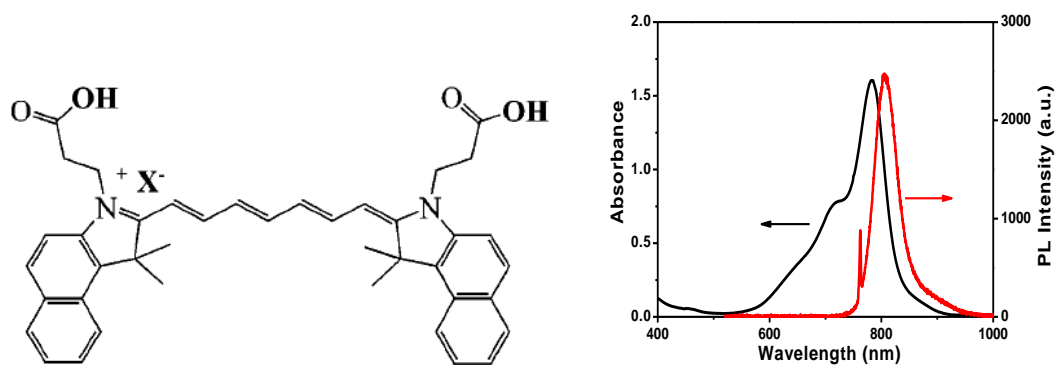


Fig. S8 Left: The molecular structure of the NIR dye-cypate provided by prof. Samuel Achilefu. Right: Absorption and PL spectra of cypate.^{1,2}

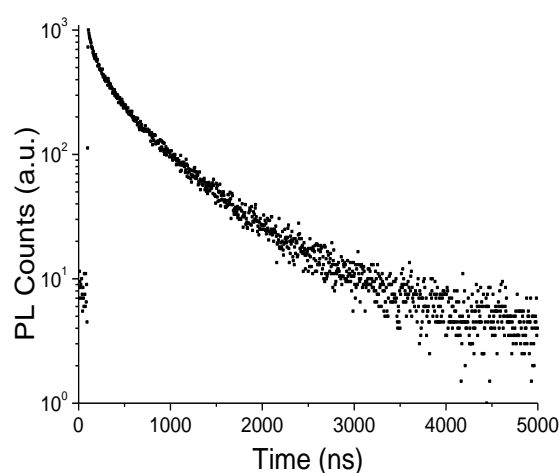


Fig. S9 PL lifetime decay of the quaternary ZnAgInSe₃ QDs sample recorded at the corresponding maximum emission wavelength (λ_{em} =680 nm) under excitation wavelength of 405 nm. Similar to previous reports,¹²⁻¹⁴ the quaternary I-III-VI-based QDs prepared in this study also have a long PL lifetime (hundreds of nanoseconds).

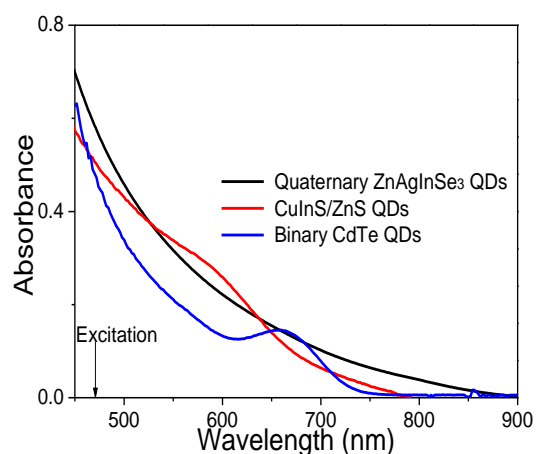


Fig. S10 Absorption spectra of quaternary ZnAgInSe_3 , CuInS/ZnS and binary CdTe QDs studied. Their PL spectra were shown in Fig. 2a.

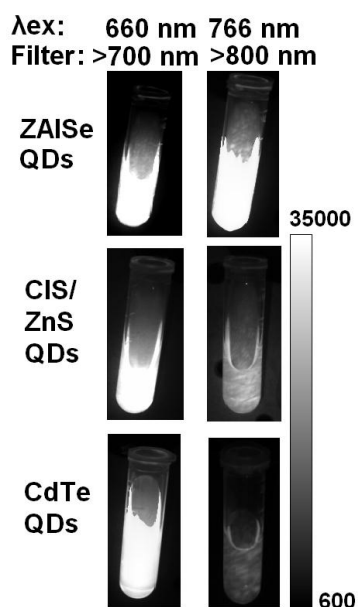


Fig. S11 The digital black and white images of quaternary ZAISe QDs, CuInS/ZnS QDs and binary CdTe QDs taken under the excitations of 660 nm and 766 nm. The corresponding pseudocolored images were shown in Fig. 2b.

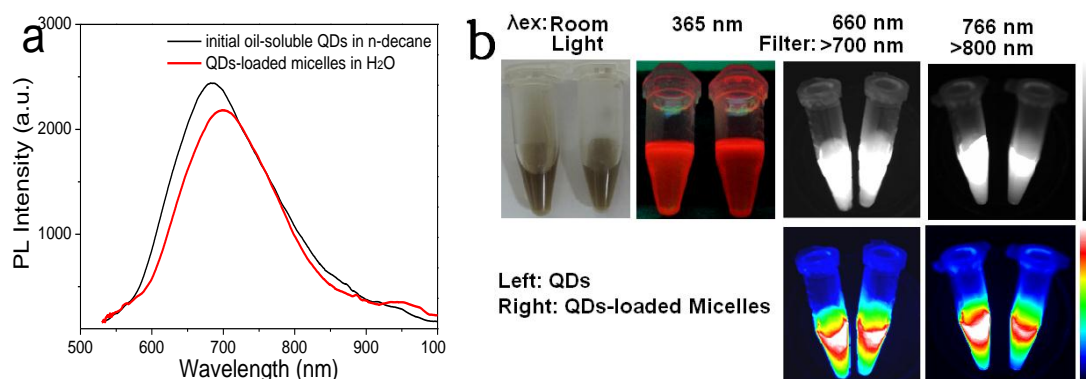


Fig. S12 (a) PL spectra of initial oil-soluble quaternary ZAISe QDs in n-decane and after transfer into water *via* FA-SOC micelles. (b) The digital images of the three QD samples taken under room light, UV lamp, the excitations of 660 nm and 766 nm.

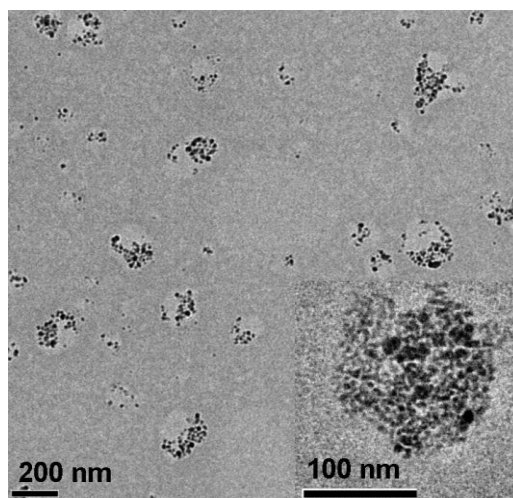


Fig. S13 The TEM image of the QDs-loaded micelles. Inset is a higher magnification TEM image of a QDs/micelle nanocomposite.

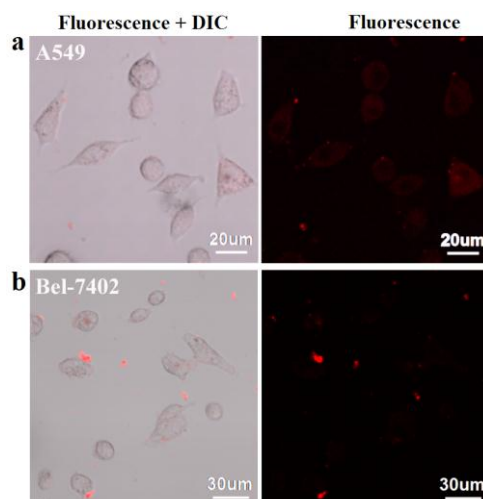


Fig. S14 (a) Optical microscopy of live FA receptor-negative A549 cells incubated with QDs-loaded FA-SOC micelles: (left) fluorescence+differential interference contrast (DIC) and (right) fluorescence image (quaternary QDs-loaded micelles, $\lambda_{\text{ex}} = 488 \text{ nm}$). (b) Optical microscopy of live FA receptor-positive Bel-7402 cells incubated with QDs-loaded SOC micelles (without FA functionalization): (left) fluorescence+DIC and (right) fluorescence image (quaternary QDs-loaded micelles, $\lambda_{\text{ex}} = 488 \text{ nm}$).

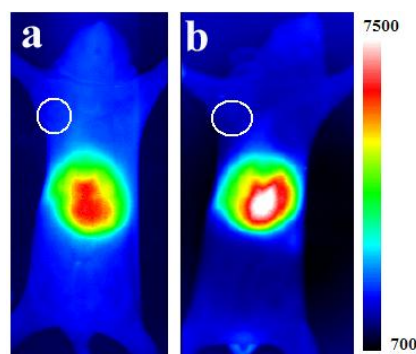


Fig. S15 (a) NIR fluorescence image of FA receptor-negative A549 tumor-bearing nude mouse after intravenous injection with the QDs-loaded FA-SOC micelles acquired at 6 h post-injection; (b) NIR fluorescence image of FA receptor-positive Bel-7402 tumor-bearing nude mouse after intravenous injection with the QDs-loaded SOC micelles (without FA functionalization) acquired at 6 h post-injection ($\lambda_{\text{ex}}=660 \text{ nm}$, an 800-nm long-pass filter). The tumor site is indicated by white circle.

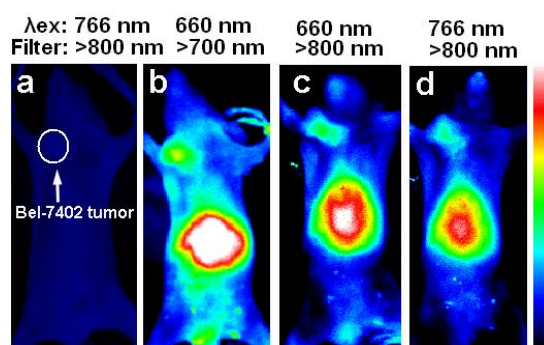


Fig. S16 NIR fluorescence images of FA receptor-positive Bel-7402 tumor-bearing nude mouse before injection (a) and after intravenous injection with the QDs-loaded FA-SOC micelles for 4 h: (b) $\lambda_{\text{ex}}=660$ nm, a 700-nm long-pass filter; (c) $\lambda_{\text{ex}}=660$ nm, a 800-nm long-pass filter, (d) $\lambda_{\text{ex}}=766$ nm, an 800-nm long-pass filter. The tumor site is indicated by white circle. As compared with the NIR fluorescence imaging of the QDs (Fig. 2b) and the QDs-loaded micelles (Fig. S11) samples in eppendorf tubes, the in vivo NIR imaging of nude mouse is much more complicated because the autofluorescence from tissues at 660 nm excitation will confound the fluorescence imaging (Fig. S13). As shown in Fig. S13, the detected tissue autofluorescence can be minimized by changing the excitation wavelength to 766 nm or selecting an 800-nm long-pass emission filter.

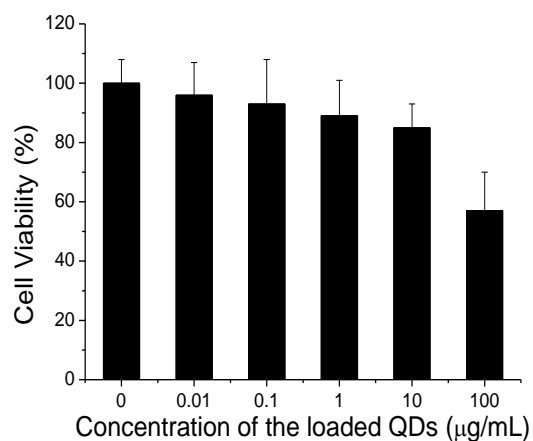


Fig. S17 Cell viability of human embryonic lung fibroblast (HEL) cells incubated with different concentrations of QDs-loaded FA-SOC micelles ($[\text{QDs}]=0, 0.01, 0.1, 1, 10$, and $100 \mu\text{g/mL}$) for 48 h. Here, MTT assay was conducted to assess preliminarily the cytotoxicity of QDs-loaded FA-SOC Micelles. The OD was measured with a Microplate Reader (Biorad).

REFERENCES

- 1 Y. P. Ye, S. Bloch, J. Kao and S. Achilefu, *Bioconjugate Chem.*, 2005, **16**, 51–61.
- 2 Y. P. Ye, S. Bloch, B. Xu and S. Achilefu, *Bioconjugate Chem.*, 2008, **19**, 225–234.
- 3 D. W. Deng, Y. Q. Chen, J. Cao, J. M. Tian, Z. Y. Qian, S. Achilefu and Y. Q. Gu, *Chem. Mater.*, 2012, **24**, 3029–3037.
- 4 H. Y. Zhu, F. Liu, J. Guo, J. P. Xue, Z. Y. Qian and Y. Q. Gu, *Carbohydr. Polym.*, 2011, **86**, 1118–1129.
- 5 Y. Liu, D. Yao, L. Shen, H. Zhang, X. Zhang and B. Yang, *J. Am. Chem. Soc.*, 2012, **134**, 7207–7210.
- 6 M. Grabolle, M. Spieles, V. Lesnyak, N. Gaponik, A. Eychmüller and U. Resch-Genger, *Anal. Chem.*, 2009, **81**, 6285–6294.
- 7 J. Zhang, H. Y. Chen, L. Xu and Y. Q. Gu, *J. Control. Release*, 2008, **131**, 34–40.
- 8 H. Z. Zhong, Z. L. Bai and B. S. Zou, *J. Phys. Chem. Lett.*, 2012, **3**, 3167–3175.
- 9 J. Cao, B. Xue, H. Li, D. W. Deng and Y. Q. Gu, *J. Colloid Interface Sci.*, 2010, **348**, 369–376.
- 10 R. G. Xie, M. Rutherford and X. G. Peng, *J. Am. Chem. Soc.*, 2009, **131**, 5691–5697.
- 11 G. D. Moon, S. Ko, Y. Min, J. Zeng, Y. N. Xia and U. Jeong, *Nano Today*, 2011, **6**, 186–203.
- 12 J. Zhang, R. G. Xie and W. S. Yang, *Chem. Mater.*, 2011, **23**, 3357–3361.
- 13 X. S. Tang, K. Yu, Q. H. Xu, E. S. G. Choo, G. K. L. Goh and J. M. Xue, *J. Mater. Chem.*, 2011, **21**, 11239–11243.
- 14 X. S. Tang, W. Cheng, E. S. G. Choo and J. M. Xue, *Chem. Commun.*, 2011, **47**, 5217–5219.
- 15 D. W. Deng, J. Cao, L. Z. Qu, S. Achilefu and Y. Q. Gu, *Phys. Chem. Chem. Phys.*, 2013, **15**, 5078–5083.
- 16 B. Xue, D. W. Deng, J. Cao, F. Liu, X. Li, W. J. Akers, S. Achilefu and Y. Q. Gu, *Dalton Trans.*, 2012, **41**, 4935–4947.
- 17 D. W. Deng, J. Cao, J. F. Xia, Z. Y. Qian, Y. Q. Gu, Z. Z. Gu and W. J. Akers, *Eur. J. Inorg. Chem.*, 2011, 2422–2432.